ORKUSTOFNUN
NATIONAL ENERGY AUTHORITY
GEOTHERMAL DIVISION

ATLANTAL ALUMINIUM SMELTER
Subsurface exploration
Appendix C:
A seismic refraction survey

Karl Gunnarsson

OS-92055/JHD-30 B December 1992

ORKUSTOFNUN - National Energy Authority
Geothermal Division

ATLANTAL ALUMINIUM SMELTER
Subsurface exploration
Appendix C:
A seismic refraction survey

Karl Gunnarsson

OS-92055/JHD-30 B December 1992

Survey conducted for:
Hönnun Consulting Engineers
Stapi Geological Services
RFS Contractors

LIST OF CONTENTS

LIST OF FIGURES

LIST OF TABLES

1. INTRODUCTION

This report describes the data acquisition and interpretation of a seismic refraction survey of the proposed site for the Atlantal Aluminium Smelter at Keilisnes SW-Iceland. The work was carried out by Orkustofnun (The National Energy Authority - Geophysics section) for the Hönnun/Stapi/RFS Joint Venture. The survey involves a single 800 m long profile, referred to as RF2 on the project maps.

According to the specifications issued for the work ("Exhibit D" of the relevant contract papers, paragraph 9.2), the survey was to define:

- Bedrock contact.
- Geotechnical conditions for excavation.
- Elastic constants for preliminary dynamic analysis for smelter facilities.
- Provide data for alternative method for estimating modules of deformation for static settlement analysis.

The area is covered by a compound basalt lava flow, that was known to be at least 25 m thick. Only thin patches of soil are found on top. As this lava can be considered as "bedrock", our survey was primarily designed to map the P-wave velocity distribution of the lava. In particular, we were on the look-out for pockets of low velocity, approaching the velocity in air, which would indicate caves or piles of volcanic slag burried within the solid lava.

2. DATA AQUISITION

2.1 Preliminary tests

Some seismic refraction tests were carried out at the Keilisnes site in August 1992, in order to get a rough idea of the structure of the area, and to evaluate what kind of signal sources would be required. Explosions were made in the deep hole KK-5, in 1 m deep boreholes in the rock, and in the soil. The results indicated that this site was rather difficult for the seismic method, and had the following characteristics:

1) The P-wave velocity of the lava pile is very low and variable, but increases below the water table. No late arrivals were observed, which indicated that the seismic reflection method would be unfeasible, and the detection of S-waves unlikely.

2) The attenuation of the seismic wave was seen to be great, considering that the beds are classified as solid igneous rocks. High frequencies were practically absent from the signal, and first arrivals had emergent character, making accurate time picks difficult to obtain beyond about 100 m ranges.

3) It was obvious that light energy sources such as hammers would be useless, and even a 2 kg high explosives charge burried in the shallow soil layer was insufficient. The best results were obtained from the deep placement of a charge in hole KK-5, which reached below the water table.

Table 1. Shot parameters for profile RF2 (grouped by "spreads").

borehole	location (m)	sp. no.	rec. no.	depth (m)	charge (kg)	sp. no.	rec. no.	depth (m)	charge (kg)
PH-21	101.1	4	52	11.7	0.8				
SRH-2	131.1	4	53	2.0	0.4				
PH-22	154.8	4	51	14.8	0.8				
SRH-3	179.5	4	50	2.0	0.4				
PH-23	203.8	4	49	14.1	0.8				
SRH-4	229.7	4	48	2.0	0.4				
PH-24	255.2	4	47	14.0	0.8				
SRH-5	280.0	4	46	2.0	0.4				
CH-3*	306.5	4	45	22.8	0.8	3	43	25.5	1.6
SRH-6	333.5					3	42	2.0	0.8
PH-25	358.7	4	44	10.2	0.8	3	41	14.3	1.6
SRH-7	384.1					3	40	2.0	0.8
PH-26	410.0					3	39	14.0	1.6
SRH-8	436.7					3	37	2.0	0.8
PH-28	460.9					3	36	10.9	1.6
SRH-9	488.3					3	35	2.0	0.8
CH-4	512.0					3	34	19.5	1.6
PH-29	564.7	2	32	11.2	1.6	3	33	7.5	1.6
SRH-11	588.3	2	31	2.0	0.8				
PH-31	614.0	2	30	14.8	1.6				
SRH-12	642.6	2	29	2.0	0.5				
PH-32	666.1	2	28	13.7	1.4				
SRH-13	694.1	2	27	2.0	0.5				
PH-33	717.6	2	26	13.4	1.4				
SRH-14	743.2	2	25	2.0	0.5				
CH-5**	768.7	2	24	25.0	1.4	1	23	25.0	1.8
SRH-15	795.8					1	22	2.0	0.5
PH-34	818.5					1	21	14.2	1.4
SRH-16	846.0					1	20	2.0	0.5
PH-36	871.0					1	19	14.6	1.4
SRH-17	899.9					1	12	2.0	0.5
KK-5	924.7					1	18	15.0	1.4
SRH-19	950.4					1	14	2.0	0.5
PH-37	974.8					1	17	9.8	1.0
SRH-20	998.3					1	16	2.0	0.5

*) Ground water level at depth 20.5 m
**) Ground water level at depth 20.0 m

2.2 Field work

The survey was carried out between October 19 and 23, 1992. Based on the results of the preliminary tests, it was decided to utilize the deep exploratory boreholes for the placement of the shots (the explosive charges). These holes were placed along the survey profiles at 50 m intervals. This was an ideal situation for tackling this difficult site. In order to get a better measure of the velocity at the surface, 2 m deep shotholes were drilled in between the deep holes, thus providing a shot location at every 25 m. High explosives charges ranging from 0.5 to 1.8 kg were used. The charges were confined using water or sand, the latter giving the best results.

Four geophone spreads were laid along the line RF2. Each spread consists of 24 geophones placed at 10 m intervals, measuring 230 m between ends. The spreads overlapped by 10 or 20 m. For each spread about 10 shots were fired. Exact information about shot positions and parameters is shown in table 1.

The recording instrument was an EG&G Geometrics ES-2401 24 channel instrument. The records are stored on 3.5" diskettes. The geophones were Mark, 10 Hz. The main recording parameters are:

- Number of channels: 24
- Recording time: 204 ms
- Sampling interval: 0.2 ms
- Band pass filter: 50-1000 Hz

3. INTERPRETATION METHODS

3.1 General approach

The intrepretation of the seismic refraction data for the lava pile is based on a simple model consisting of two layers. The dry lava, about 20 m thick, is represented by the upper layer, and the water saturated lava below the ground water table is the lower layer, the refractor. We will refer to these layers as layers 1 and 2.

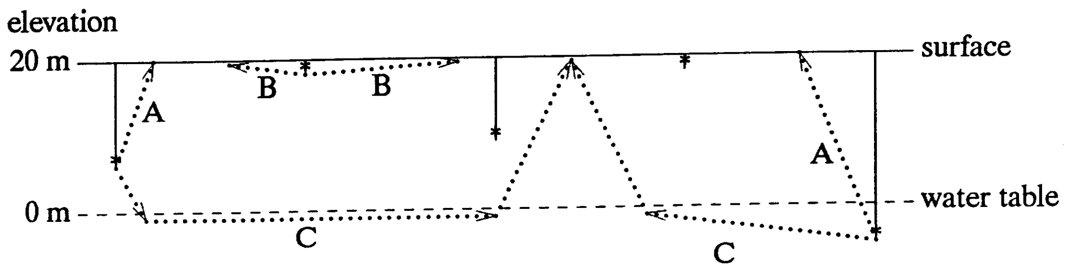

Figure 1. A schematic cross section indicating the various types of seismic ray paths (dotted lines) used for defining the velocity structure of the lava pile. Rays "A" are up-hole arrivals, rays "B" are the direct horizontal wave, and "C" represents the refracted wave from the water saturated lava. Boreholes and shot locations are indicated by vertical lines and asteriks.

In principle, the interpretation is based on three types of travel paths or "rays" of the seismic wave, as is shown scematically in figure 1:

1) Near vertical or steeply dipping rays ("A" in figure 1) pass from the deep shot positions up to the surface, giving a measure of the velocity for the direct wave passing up through the lava pile (layer 1). We can assume that these rays sample a triangular shaped area in the section, with the point at the shot location and the base along the surface to a distance roughly equal to the depth of the shot. As the holes usually penetrate to the lower part of the upper layer, these measurements give a good estimate for the average velocity up through the layer at that location.

2) Horizontal direct wave rays ("B") pass from the shallow shot holes along the surface, giving a measure of the velocity in the uppermost part of the upper layer, in the regions in betwen the deep holes.

3) The ray corresponding to the refracted head wave from the deep shots ("C") passes down to the interface between the upper and lower layers, along the interface and then up to the surface geophone positions beyond the critical distance. A unique solution for the velocity of the lower layer can be obtained by using reversed ray paths of this type. The well known GRM-method (Generalized Reciprocal Method) is used for this purpose. Results of this analysis include the velocity of the refractor, and a delay time term, as a function of distance along the profile. The time delay is a measure of the depth to the refractor, which can be determined if the velocity of the surface layer is known.

This experimental sceme provides a fairly comprehensive coverage of the P-wave velocity structure of the lava formations. The lower part of the upper layer is not comprehensively sampled by the direct waves, and as the velocity is observed to vary greatly over short distances, the velocity close to the surface is not necessarily representative for the whole depth range. The delay time term calculated from the refraction solution is, however, a measure of the average velocity of the entire upper layer at each geophone station position, but is also dependent on the depth to the interface (refractor). This leads to two possible interpretation scemes:

1) A likely velocity model can be constructed for the upper layer from the direct wave information. Using this velocity model, the delay times can be converted into depth to the refractor along the profile.

2) An alternative approach is to assume that the depth to the refractor is known, i.e. the interface coincides with the ground water table, and calculate average velocity for the upper layer, as a function of distance along the profile. By comparing this average velocity with the velocity measured by the direct wave close to the surface, it is possible to deduce deviations in velocity in the lower part of the layer.

The second alternative is our favoured approach, and the results indicate that it is generally valid.

3.2 The interpretation sequence

Each spread of 24 geophones, 230 m long, has been interpreted independently, but with due regard to the adjacent spreads at the overlapping ends. The data processing and interpretation sequence is in general as follows:

1. The shot records are transferred to a PC computer, and read into the program FIRSTPIX (Interpex ltd.) , which allows to read the time of the first breaks (seismic arrivals) of the records, and to enter the positional information. The output consists of tables and plots of travel times and distances (locations).

2. After careful checking and editing, the travel time data are entered into the program GREMIX (Interpex ltd.) which performs the preliminary GRM-analysis. At this stage a rough solution is obtained.

3. The direct wave times from the shallow shots close to the surface, are analyzed by linear regression to provide a velocity value to both sides of each shot location. This velocity is representative for the uppermost 5 m (or so) of the lava pile, and out to some 20-30 m away from the hole. These data are also analyzed to provide a velocity values between each geophone pair, i.e. at 10 m intervals. This approach gives large variations in velocity that could partly be due to observation errors, but indicate also greater small scale variability of the material.

4. The travel times for the direct wave from the deep shots up to the surface is analyzed to provide information on the shallow velocity structure. Two phones on each side are included in this analysis, providing steep rays, and a measure of vertical velocity.

5. By using the upper layer velocities and the refractor velocity from the preliminary GRM-solution, the travel times from each shot to the other shot locations can be corrected for the deep location of the shots, thus providing a consistent set of "reciprocal times". These times are required for correct depth estimates. Where direct measurements of rays between shot locations are not observed, the reciprocal times are obtained by the method of "phantomning". This means that overlapping parallel travel time segments are used to extrapolate the travel time curves.

6. A final GRM solution is then carried out. This time the data are edited to contain only the most reliable and consistent arrival from the refractor (lower layer), and a more detailed analysis is made for the refractor velocity. The output from this analysis consists primarily of two variables, the refractor velocity and the delay term, which are a function of position along the profile.

3.3 Interpretation of deep basement arrivals

A seismic phase from a deeper boundary is observed in all parts of the profile at ranges beyond about 100 to 130 m from the shot points, mostly as later arrivals. This phase is clearly a refracted wave from a layer or "basement" of higher velocity that lies below the lavas. The observed travel time curves are not properly reversed, and are therefore unsuitable for GRM-interpretation. This seismic phase has been interpretated assuming a horizontally layerd model. The results indicate that this simple model is sufficient to account for the observations.

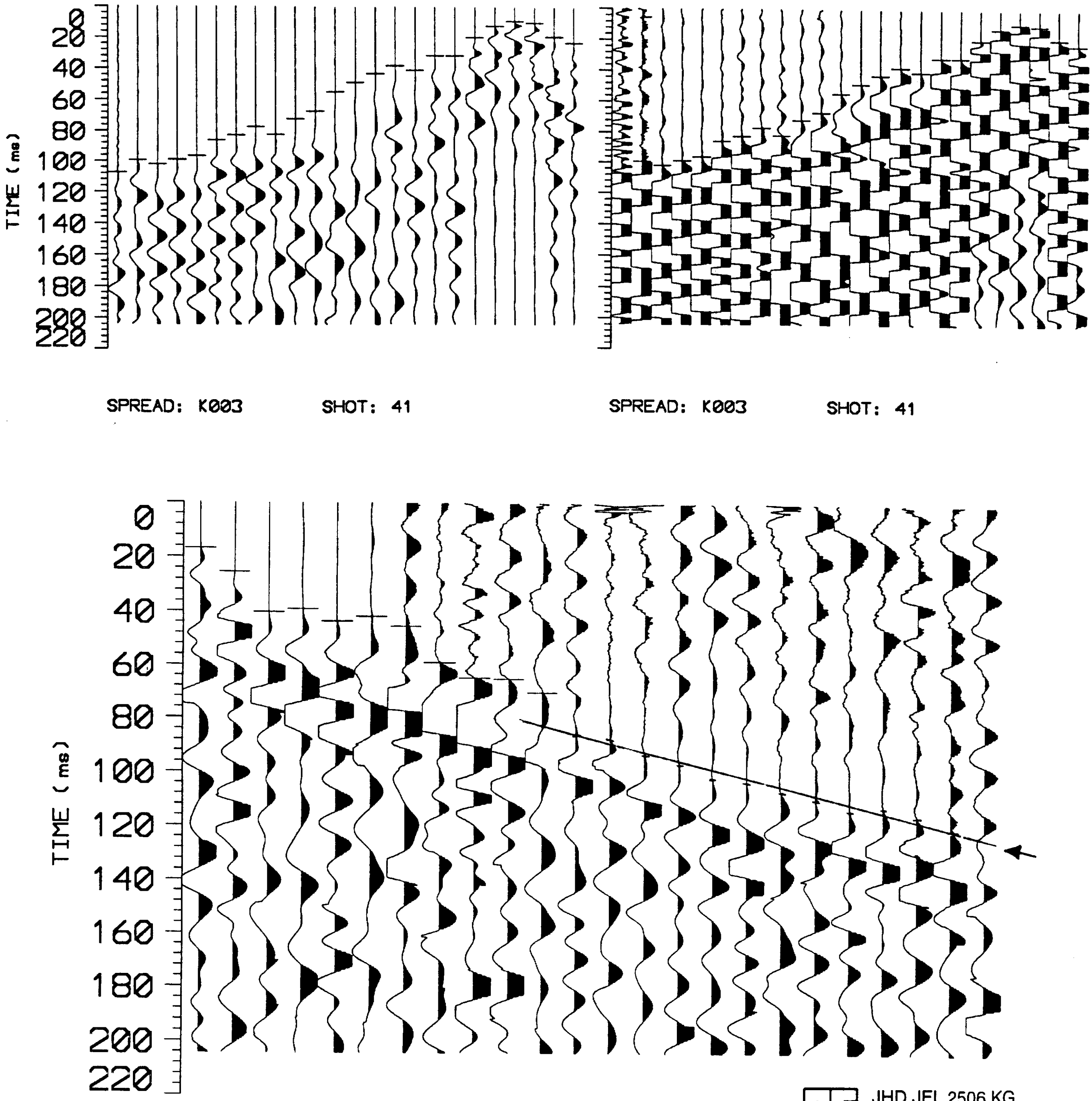

JHD JEL 2506 KG
92.12.0924 T

Figure 2. Samples of the seismic records. a) Record (shot) 41, Spread 3. The amplitude scaling is such that the whole wave sequence is represented. b) The same record with much greater amplitude gain. Note the appearance of the first breaks in the latter. c) Record 44, Spread 4. The deep basement refractor (layer 3; about 3100 m/s) is clearly identified on this record.

4. RESULTS

A typical seismic records is shown in figure 2. The difference in the signal gain of the plots show that the first arrivals are weak but distinct up to distances of about 100 m. Only such reliable time picks are used for solution of the lava refractor (layer 2). The geometry of the survey is such that complete reversed coverage is obtained with these data

Note that the horizontal distance or location parameter is referred to an arbitrary point at the western end of the profile, and distance increases to the east along the profile. The local plant coordinates have the "east-west" axis parallel to the line, and the zero of that coordinate system corresponds to 588 m on our distance axis.

The results of the interpretation procedure is presented separately for each of the four geophone spreads. For each spread the following four graphs are presented:

1) A composite travel-time diagram showing all observed first arrivals.

2) A composite travel-time diagram showing only a selected sub-set of the data used for the the GRM-analysis of the lower lava layer (the layer 2 refractor). These data consist only of records from shots in deep boreholes, as they generally provide clearer first arrivals, and the refracted phase is also observed at shorter distances. The ranges are typically restricted to less than 100 m, to avoid suspect picks at the the greater ranges. This data set provides a complete reversed coverage for the spread.

3) A delay-time versus distance (location along the profile) diagram shows the result from the GRM-analysis. These are the delay-times calculated for the upper lava layer. They are a measure of the thickness, and are also dependent on velocity. The scatter of values results from individual solutions for various overlapping pairs of travel time curves, and is a indication of the accuracy of the solution.

4) A graph of velocities as a function of distance is presented in the next diagram. The refractor velocity is the result of the GRM-analysis of the refracted phase. Three different types of upper layer velocities are presented:
(i) The velocity of the direct wave from the shallow shot holes is represented by solid lines. One value is observed to each side of every shot, and the extent of the lines shows the length of the curve segment used. This velocity is representative for the uppermost 5-10 m of the layer, and typically averages out 20 m intervals.
(ii) Another measure of the direct wave is obtained from the up-hole times from the deep shot holes. This is indicated by arrows from the shot locations (dots) to the position of the geophones. Two phones on each side of each hole are analysed.
(iii) The dotted line shows a velocity function calculated from the mean delay time function of the previous diagram, using the assumption that the refractor interface coincides with the ground water table at approximately zero elevation. This velocity should represent an average value of the entire layer.

The results are then summed up in a single cross section, that shows the velocity distribution in a schematic way.

4.1 Spread 4

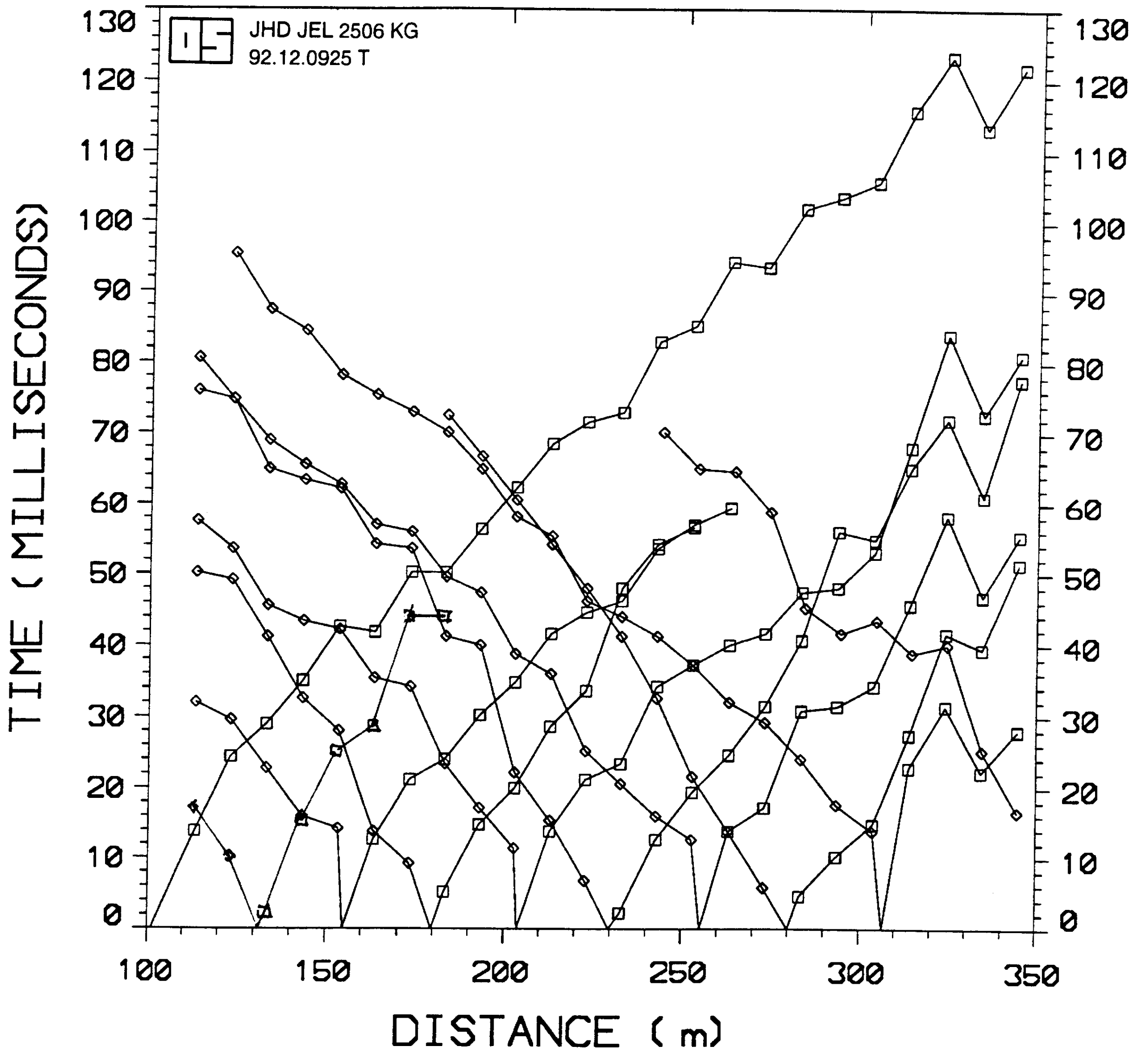

Figure 3. Travel time curves observed on Spread 4.

The refractor velocity is relatively high, indicating relatively competent rock in the lower part of the lavas, especially in the distance range 220-300 m. The upper layer shows a positive velocity anomaly between 200 and 305 and a adjacent negative anomaly in range 305-350 m, where the velocity is about 1000 m/s, not a exceptionally low value.

Figure 4 (next page). Interpretation results of Spread 4 for lava formation. a) Travel time curves used in GRM-analysis. b) Delay times or "time depth" from GRM-solution . c) Refractor velocity from GRM-solution and upper layer velocity from direct wave analysis from shallow and deep shot holes, and from the delay diagram (b).

KR04 shots: 52 51 49 47 45 44

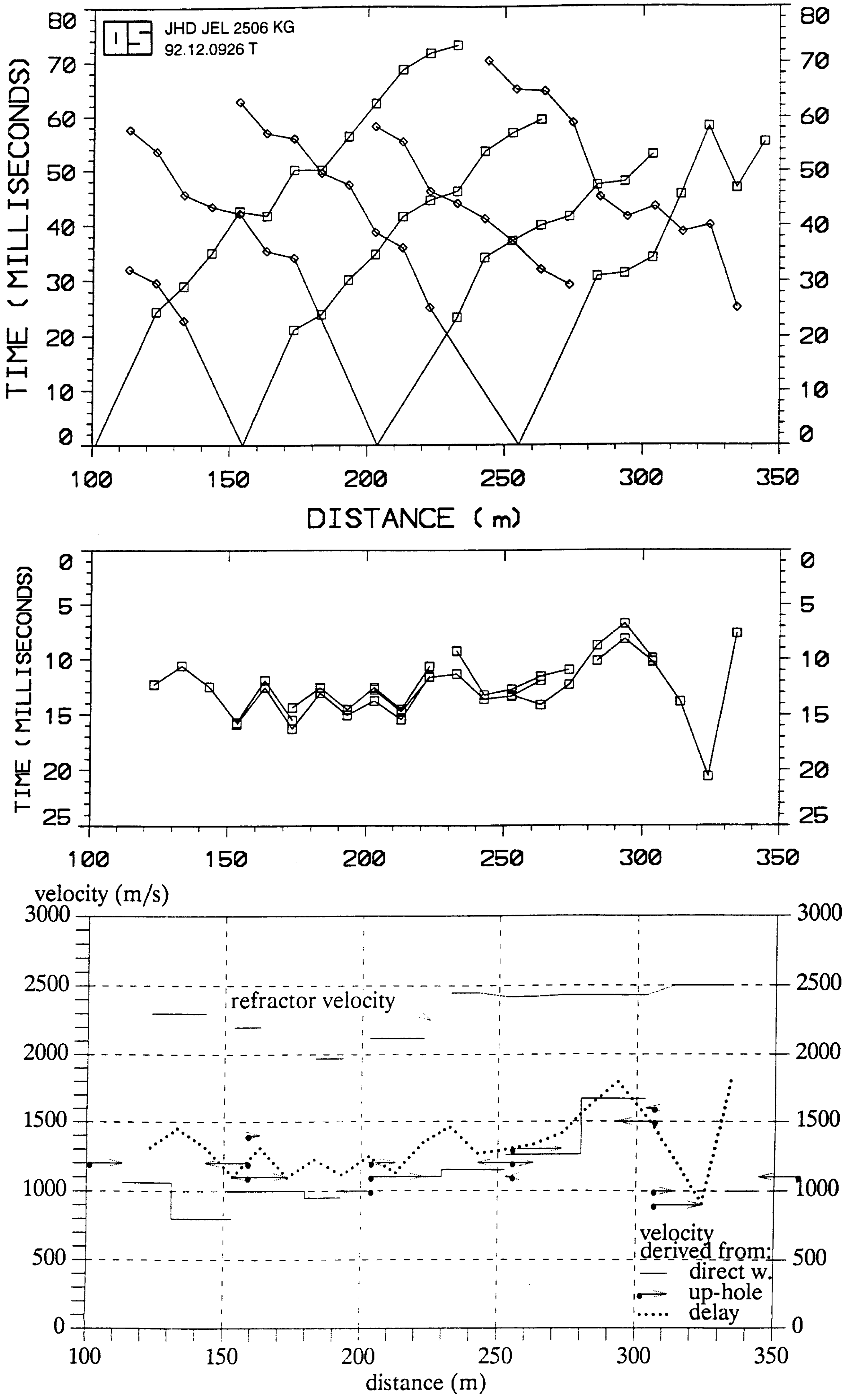

4.2 Spread 3

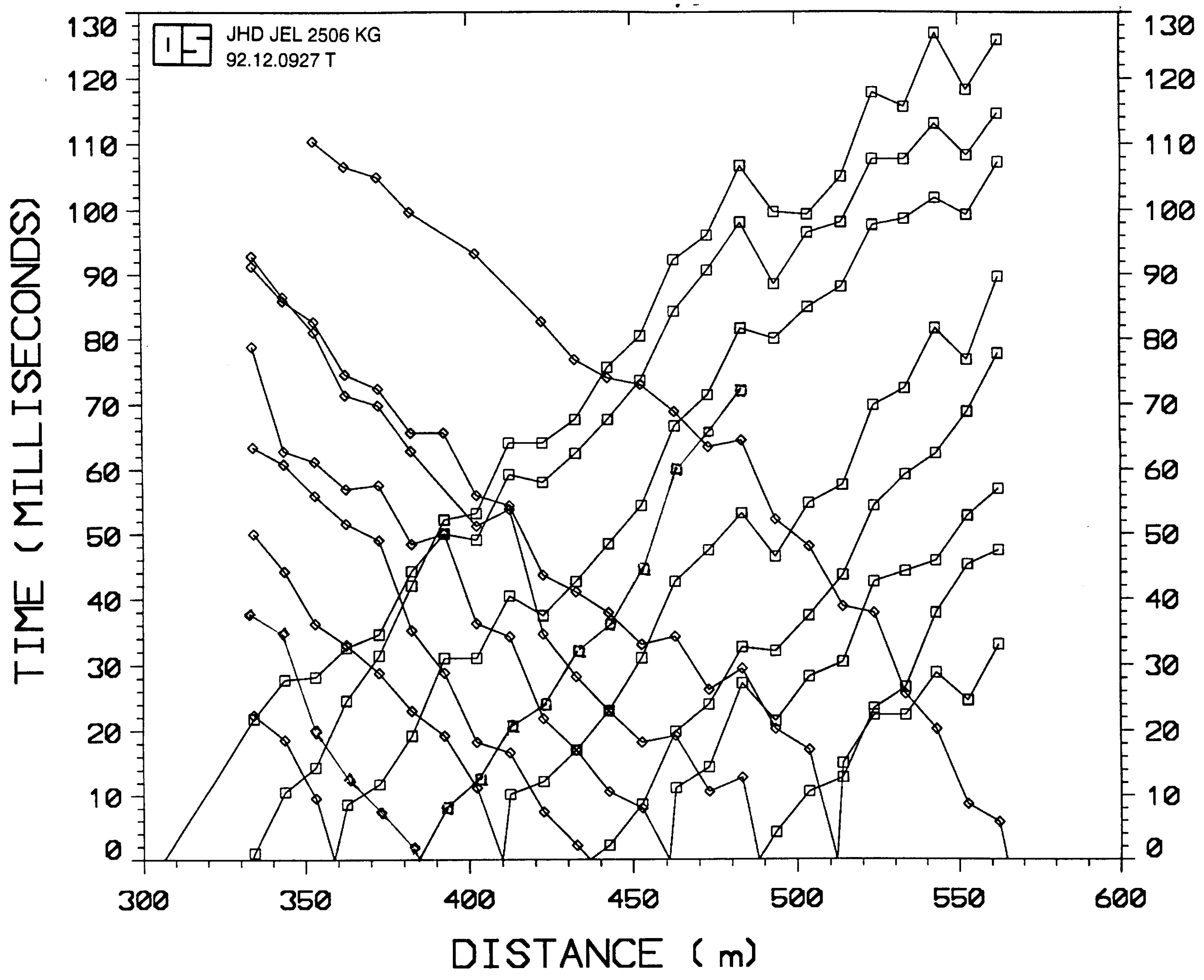

Figure 5. Travel time curves observed on Spread 3.

The upper layer shows considerable variations. A narrow zone (<10 m) at location 485 m adjacent to a shallow shot hole shows a suspiciously low velocity, approaching the velocity in air. Although a observation error can not be excluded, there could be a weekness at this place.

Figure 6 (next page). Interpretation results of Spread 3 for the lava formation. See fig. 4 for explanations.

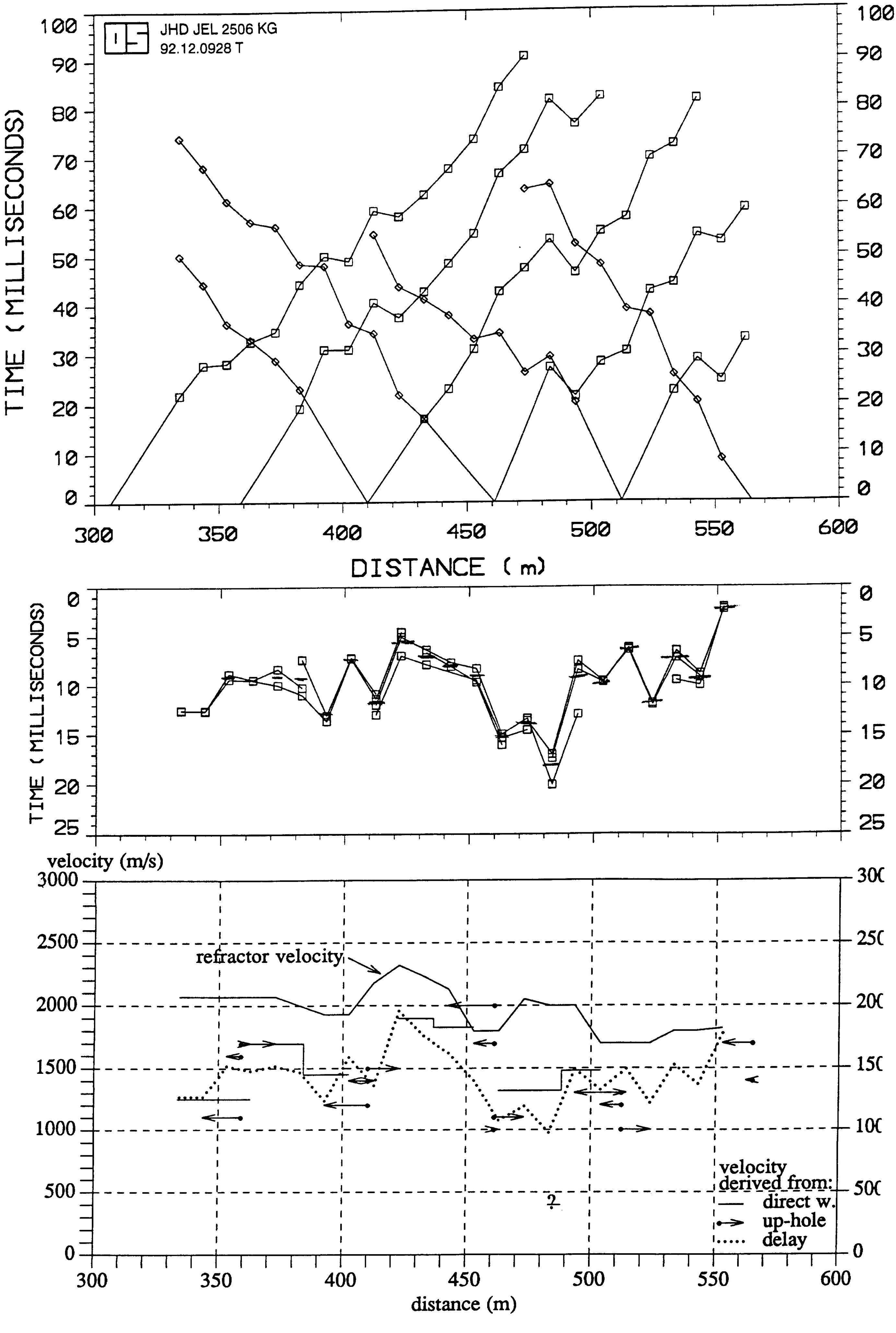
JHD JEL 2506 KG
92.12.0928 T
TIME (MILLISECONDS)
DISTANCE (m)
TIME (MILLISECONDS)
velocity (m/s)
refractor velocity
velocity derived from:
direct w.
up-hole
delay
distance (m)

4.3 Spread 2

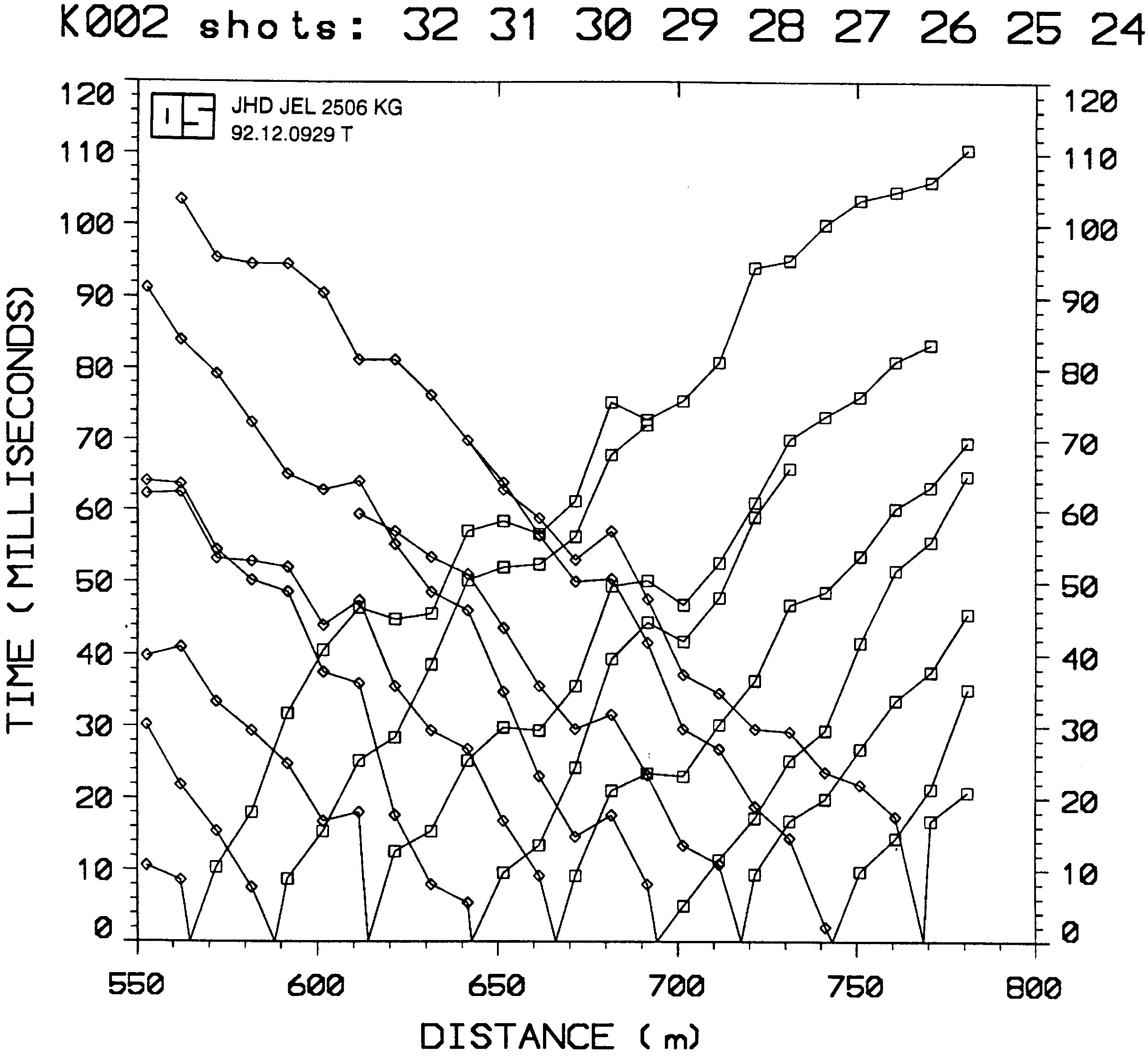

Figure 7. Travel time curves observed on Spread 2.

The upper layer velocity shows considerable variations between blocks of 10 to 30 m lateral dimensions. Two low velocity spots are seen, at 614 m (800 m/s), and at 690 m (700 m/s).

Figure 8 (next page). Interpretation results of Spread 2 for lava formation. See fig. 4 for explanations.

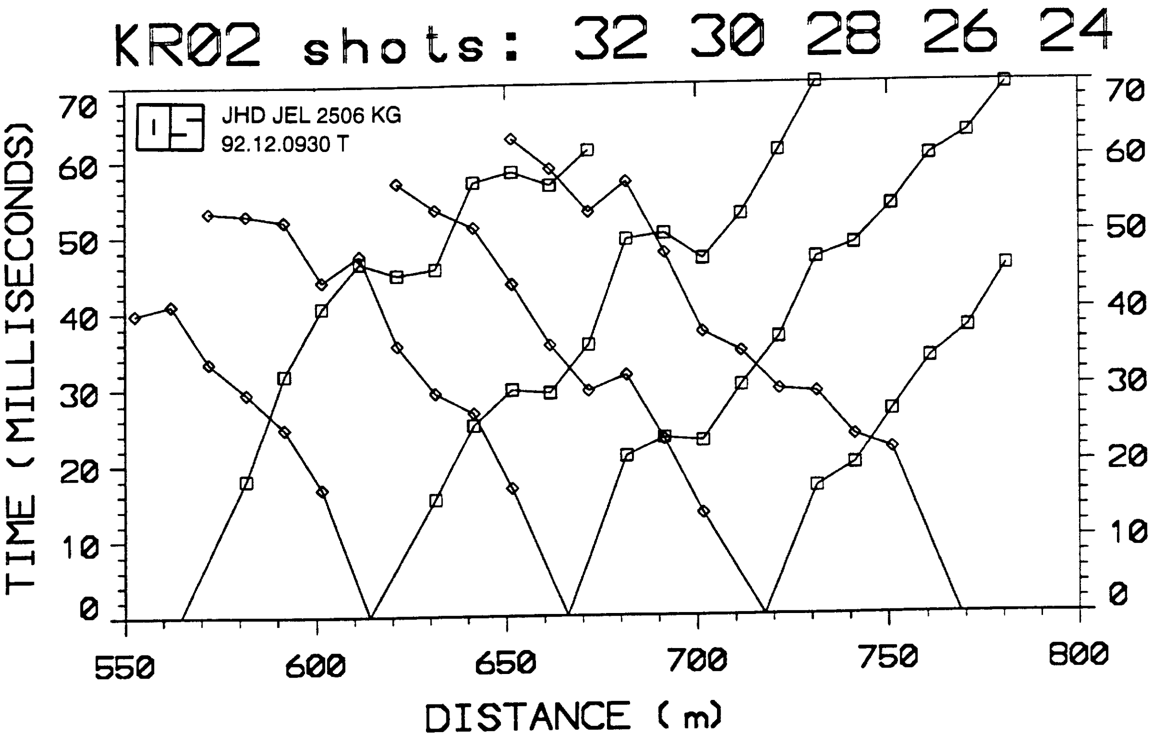
KR02 shots: 32 30 28 26 24
JHD JEL 2506 KG
92.12.0930 T
TIME (MILLISECONDS)
DISTANCE (m)

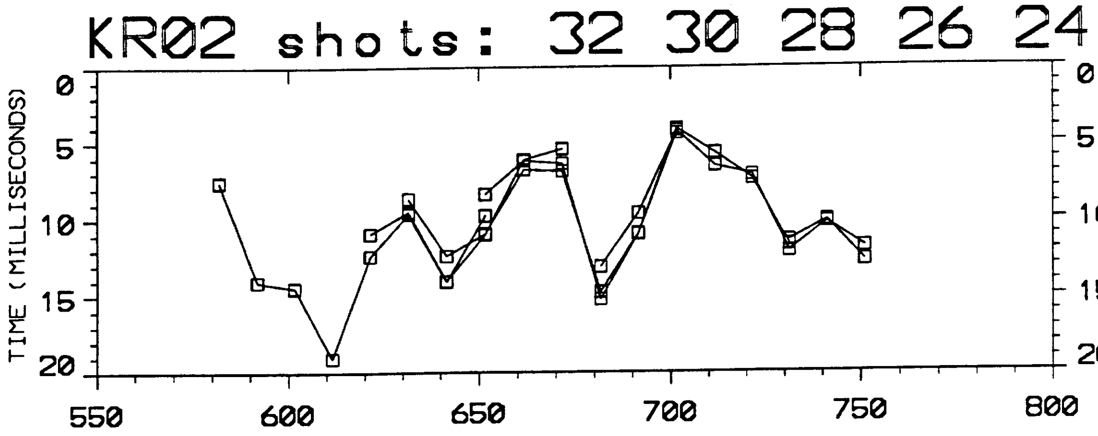
KR02 shots: 32 30 28 26 24
TIME (MILLISECONDS)

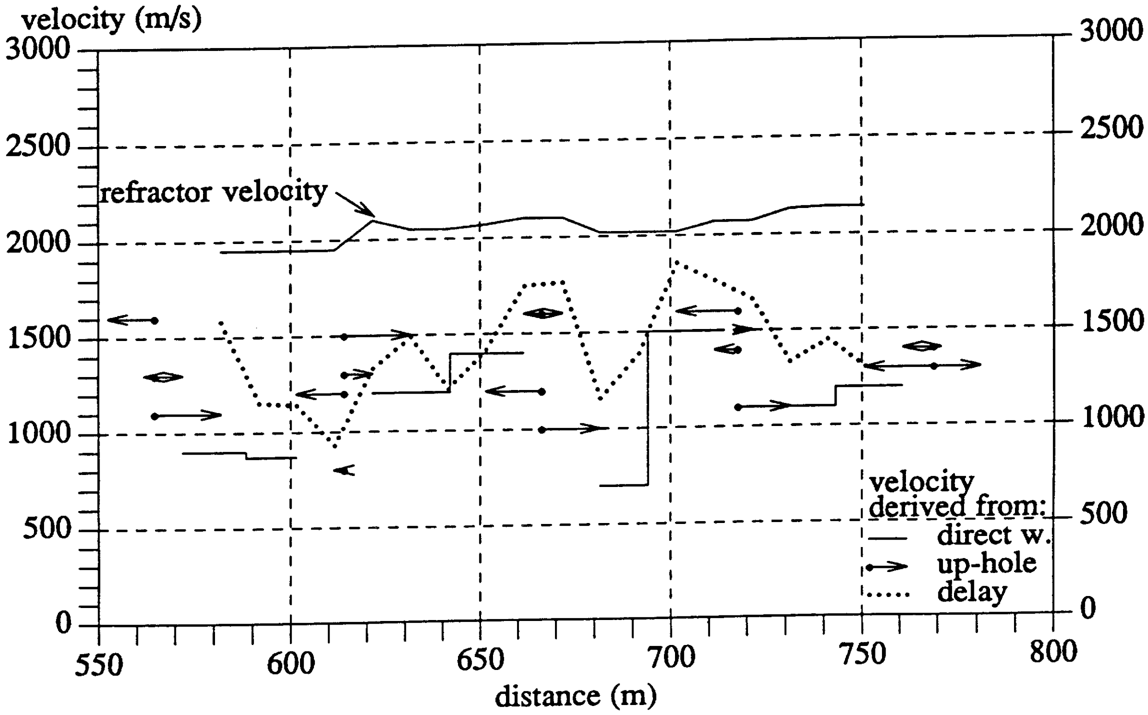
velocity (m/s)
refractor velocity
velocity
derived from:
direct w.
up-hole
delay
distance (m)

4.4 Spread 1

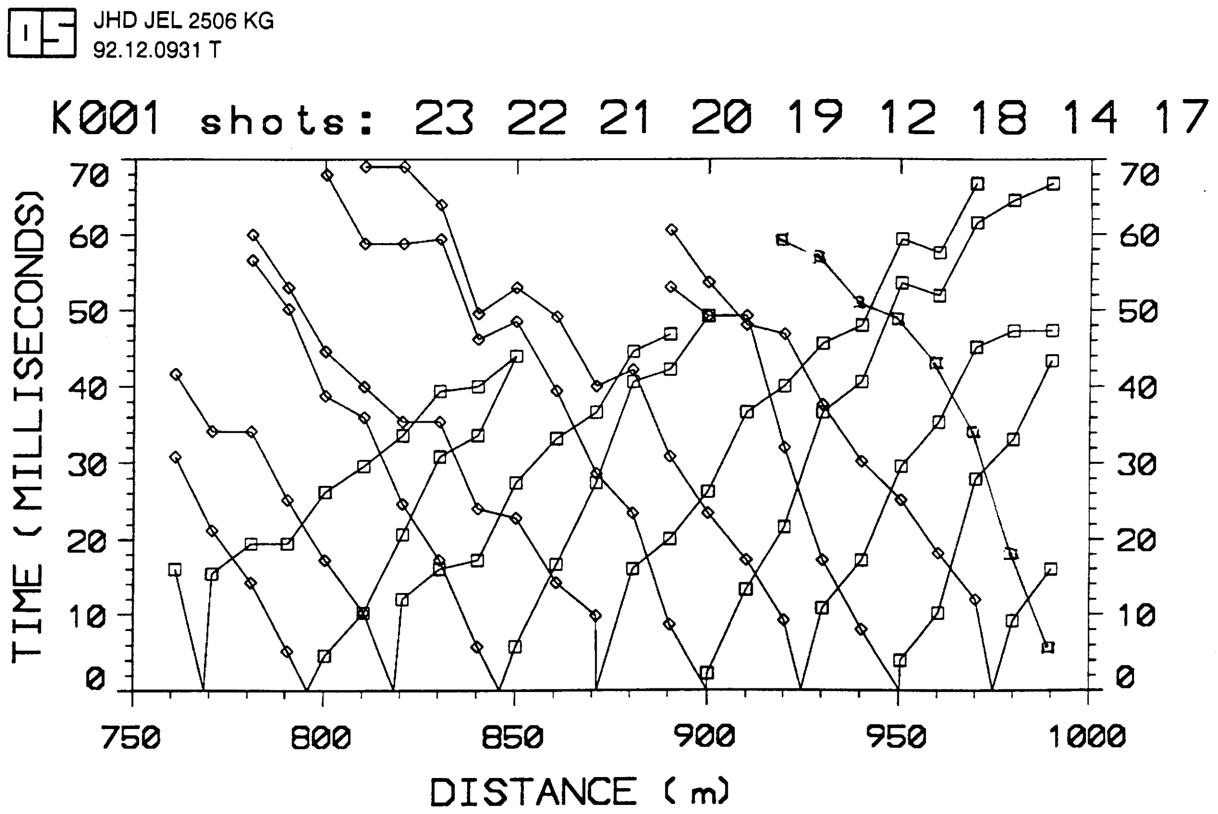

Figure 9. Travel time curves observed on Spread 1.

Velocities are here relatively low close to the surface, as compared to the lower part of layer 1. Lowest values are found at the the right end where velocities as low as 800 m/s are seen, and where the refractor velocity (layer 2) is also low.

Figure 10 (next page). Interpretation results of Spread 1 for the lava formation. See fig. 4 for explanations.

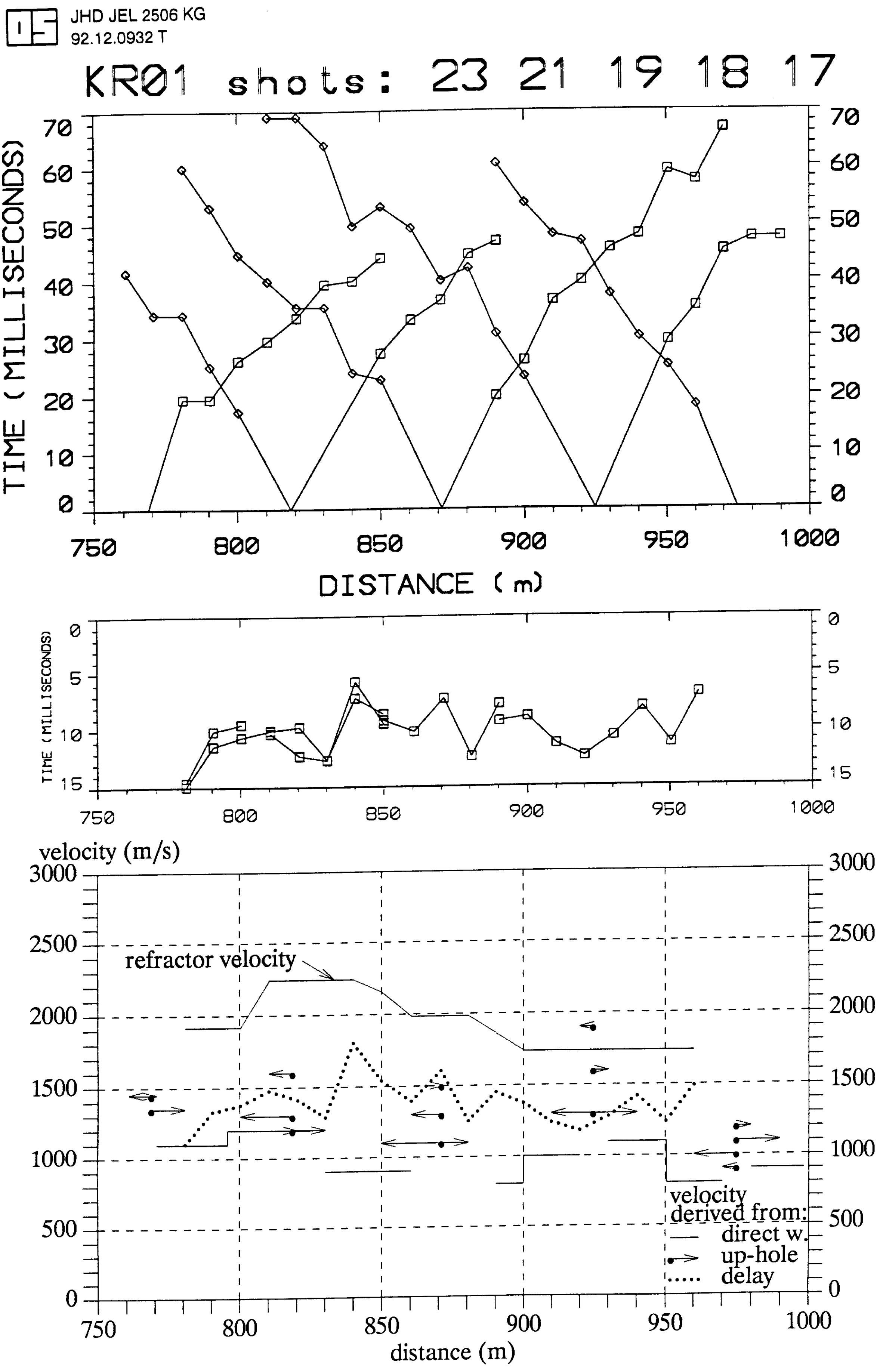
JHD JEL 2506 KG
92.12.0932 T
KR01 shots: 23 21 19 18 17
TIME (MILLISECONDS)
DISTANCE (m)
TIME (MILLISECONDS)
velocity (m/s)
refractor velocity
velocity
derived from:
direct w.
up-hole
delay
distance (m)

4.5 Summary of results for the lava formation

Figure 11 shows the interpretation of the velocity structure. Representative velocity values are given at intervals in the upper lava layer (dry), and blocks of high velocities (dotted) and low velocity (hatched) are shaded. The low velocity areas have values below 1000 m/s and the high velovity areas above 1500. The shallow direct wave shows typically slightly lower values than the delay-derived velocity, indicating some velocity increase with depth, and this has been estimated as is shown in the section. The inhomogeneiity of the lava is clearly shown in the rapid variation in velocity. The values are typically averaged over 10 to 30 m intervals, and the velocity contrasts are in fact even greater in smaller scale structure, as the "higer resolution" deviation figures in table 2 indicate.

Table 2 shows a statistical distribution of velocity layer 1 values for the four spreads, and the whole line. Table 3 shows the statistics of the refracted phase velocities, i.e. layer 2. The mean values for the dry lava is about 1300 m/s, and 2100 m/s for the saturated lava.

Table 2. Statistics of the velocity solutions (m/s) for layer 1 (dry lava).

seismic phase	number obs.	mean	sd	min	max
			velocity		
Spread 1:					
direct wave, shallow holes	9	966	141	800	1200
direct wave deep holes	19	1307	238	900	1900
calculated from delay times	19	1381	162	1104	1803
Spread 2:					
direct wave, shallow holes	8	1108	273	700	1500
same w/higher resolution	22	1327	833	200	3900
direct wave deep holes	20	1325	217	800	1600
calculated from delay times	18	1423	259	926	1853
Spread 3:					
direct wave, shallow holes	7	1561	251	1250	1900
same w/higher resolution	21	1614	891	400	4600
direct wave deep holes	18	1405	283	1000	2000
calculated from delay times	23	1427	229	971	1956
Spread 4:					
direct wave, shallow holes	9	1110	246	800	1670
same w/higher resolution	20	1150	446	600	2200
direct wave deep holes	18	1188	174	900	1600
calculated from delay times	22	1332	219	909	1801

Table 3. Velocity of the refracted wave in layer 2 (saturated lava).

refractor velocity of:	number	mean	sd	min	max
Spread 1	19	1938	199	1736	2243
Spread 2	18	2048	65	1950	2140
Spread 3	23	1966	175	1700	2320
Spread 4	22	2301	175	1970	2500

The following low velocity spots should be noticed:

- An anomaly is in the range 305-350 m, where the velocity is about 1000 m/s, which is, however, not an exceptionally low value.
- A narrow zone (< 10 m) at location 485 m adjacent to a shallow shot hole shows a suspiciously low velocity, approaching the velocity in air. Although an observation error can not be excluded, there could be a weekness at this location.
- A narrow low velocity spots at 614 m (800 m/s)
- A low velocity region at 690 m (700 m/s).

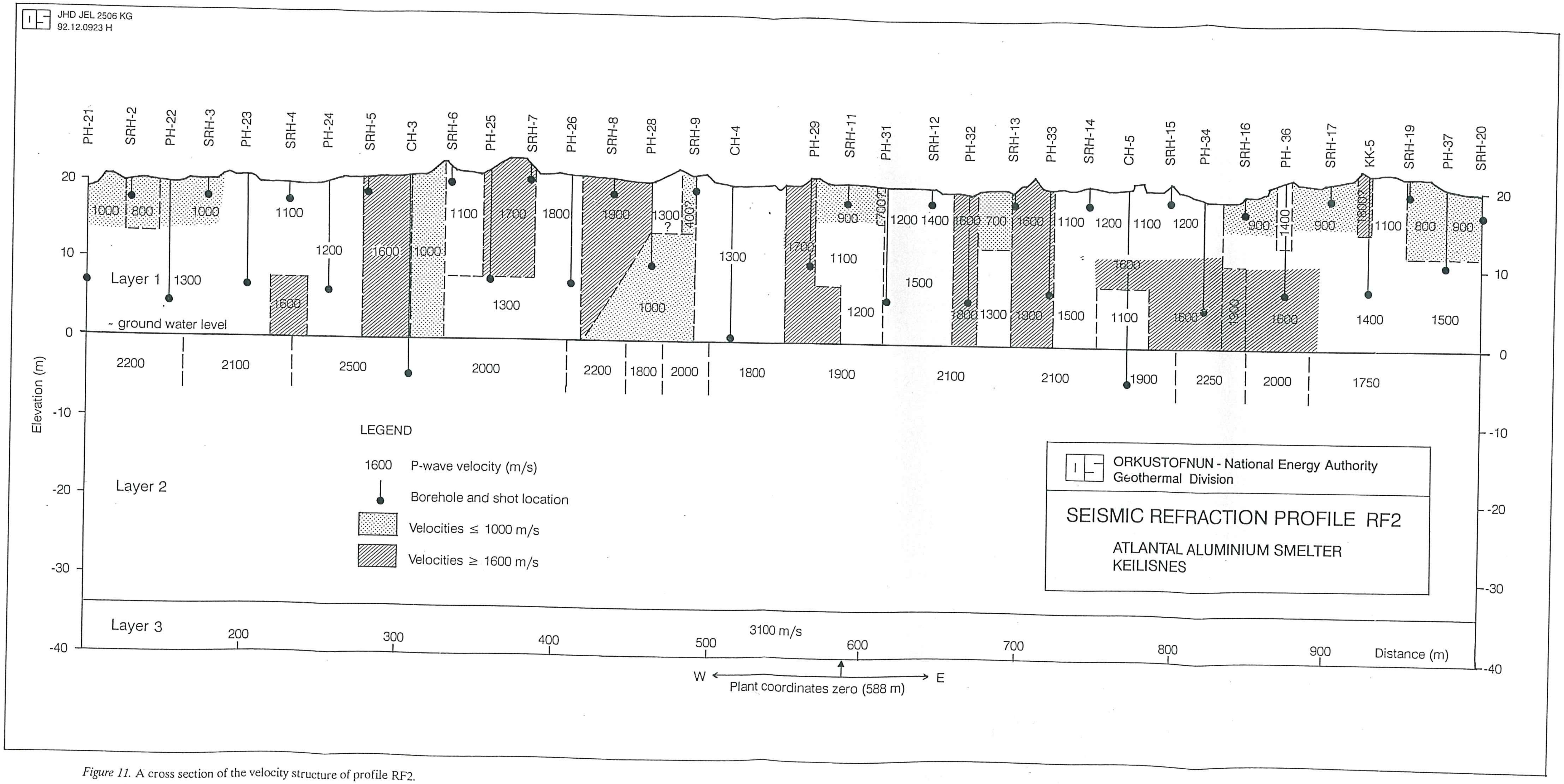

Figure 11. A cross section of the velocity structure of profile RF2.

4.6 The deep basement interface

The deep "basement" refracted phase is observed in all parts of the profile at ranges beyond about 100 to 130 m from the shot points. At the longest ranges obtained this phase comes in as first arrivals, but at shorter ranges it can be observed as a second arrival behind the lava refracted phase, due to the marked decline in energy of the latter. Although this seismic phase is relatively high in energy, the arrivals are of emergent character and therefore difficult to pick, especially where the phase is a second arrival. In many instances the first break times have been estimeted from the general shape of the wave, and are not very accurate.

Two records have been analysed for every spread, one at each end. The measured travel times are corrected for the delay at geophone station and shot location, due to the lava pile above ground water level. This procedure does in effect relate the measurements to zero elevation. The observed travel time curves consist of the refracted time curves over ranges from 110 to 240 m. The curves are interpreted by fitting straight lines to the segments, and obtaining velocity and delay times, two sets for each spread. The results of the analysis are shown in Table 4. The delay can then be converted into depth, if the velocity in the layer above the refractor is known. There is some doubt about this velocity value, as there is a possible sedimentary low-velocity layer between the surface lava and the deep refractor. We choose to use a velocity of 2000 m/s, which is close to the observed average lava velocity as measured below the water level.

Table 4. Results of analysis for deep basement refractor.

spread no	record no	hole name	velocity (m/s)	delay (ms)	depth below 0-elevation (m)
4	52	PH-21	2900	22	30
4	44	PH-25	3110	23	30
3	43	CH-3	2930	22	30
3	33	PH-29	3350	29	36
2	32	PH-29	3330	28	35
2	24	CH-5	3130	28	37
1	23	CH-5	3450	32	39
1	17	PH-37	2910	26	36
mean			3139	26	34

The average basement velocity is about 3100 m/s. The depth to the basement is calculated to be 34 m below 0-level, and deviations are less than 4 m. The uncertainties in picking travel-times and applying corrections, and in the interpretation caused the short unreversed curve segments, are such that these variations are within probable error limits, wshich are about 5 m. The results indicate that this simple interpretation scheme is sufficient to account for the observations. The calculated depth is too great if there is a pronounced low velocity layer below the lava, i.e. with velocity much less than 2000 m/s. It is, however, probable that the velocity would not be less than 1500 m/s, which would give only 10-15% decrease in the calculated depth.

5. ELASTIC PARAMETERS DERIVED FROM P-WAVE VELOCITY

5.1 Theory

The only physical parameter of the rock formations measured in this work is the compressive wave velocity or P-wave velocity (V_p). No S-wave was observed, so the S-wave velocity (V_s) is calculated from the P-velocity using the *Poisson's relation*, which is an approximation that applies fairly well for most rocks. In Iceland this has been observed to be a close approximation for basaltic rocks (Pálmason 1971). When the density of the rock is also known, the elastic parameters can be calculated. The density can bee obtained from measurements on rock samples, or it can be obtained from the the P-wave velocity using the so called *time-average function*. Thus the elastic parameter can in effect be derived from the seismic P-wave velocity alone.

The following are the usual elastic parameters:

λ: The Lamé λ parameter
μ: rigidity (Lamé parameter)
k: bulk modulus (or incompressibility)
E: Young's modulus
σ: Poisson's ratio

The elastic properties can be described by any of these pairs of parameters: λ,μ (the Lamé elastic parameters), k,μ or E,σ. We will calculate here the Young's modulus and the Poisson's ratio.

The P-wave velocity is expressed as:

$$V_p = \sqrt{\frac{\lambda + 2\mu}{\rho}} \tag{1}$$

and S-wave velocity as:

$$V_s = \sqrt{\frac{\mu}{\rho}} \tag{2}$$

The Poissons relation can be expressed by any of the following:

$$\lambda = \mu \ , \ k = \frac{5\mu}{3} \ , \ \sigma = \frac{1}{4} \ , \ V_p = \sqrt{3}V_s \ , \ V_p^2 = \frac{3\mu}{\rho} \tag{3}$$

The general expressions for the Young's modulus and Poisson's ratio are:

$$E = \frac{\mu(3\lambda+2\mu)}{\lambda+\mu} \ , \ \sigma = \frac{\lambda}{2(\lambda+\mu)} \tag{4,5}$$

When Poisson's relation applies, these equations can be simplified as:

$$E = \frac{5\mu}{2} \ , \ \sigma = \frac{1}{4} \tag{6}$$

As here is seen, the Poisson's ratio is a constant, so only the Young's modulus needs to be further considered. The parameter μ can then be substituted by a function of velocity (V_p) and density (ρ) acording to (3), to yield the expression:

$$E = \frac{5V_p^2\rho}{6} \tag{7}$$

Now we introduce the "time-average equation" to relate velocity and porosity (ϕ). This approximate relation has been used extensively, and has been shown to be applicable in Icelandic basalts (Chrisensen & Wilkens (1982); Willie, 1950).

$$\frac{1}{V} = \frac{\phi}{V_f} + \frac{1-\phi}{V_m} \ , \tag{8}$$

where V_f denotes the velocity of the fluid in the pores and V_m the velocity of the matrix material. This equation can be re-written to express porosity in terms of velocity:

$$\phi = \frac{V_f(V_m - V)}{V(V_m - V_f)} \tag{9}$$

The bulk rock density can be expressed as

$$\rho = \rho_f\phi + \rho_m(1-\phi) \tag{10}$$

By substituting for ϕ in equation (10) using eq. (9), and use the resulting equation to substitute for ρ in equation (7), the Young's modulus can be expressed as a function of observed seismic velocity only, as we can assume likely values for the rock matrix density and velocity, and the properties of the fluids are well known.

The resulting equation for Young's modulus is then as follows. The velocity denoted as "V" is understood to be the seismic P-wave velocity.

$$E = 5\frac{V^2}{6}\left[\rho_m - \frac{V_f(V_m - V)}{V(V_m - V_f)}(\rho_m - \rho_f)\right] \tag{11}$$

5.2 Calculations of porosities and elastic parameters

For calculating the typical porosity and Young's modulus of the lava formation, average velocities have been compiled for every for each of the four geophone spreads, and then for the entire profile. The following parameters are used in the calculations:

V_{air} : 340 m/s
V_{water} : 1500 m/s
V_m : 6500 m/s
ρ_{air} : 0.0 g/cm^3
ρ_{water} : 1.0 g/cm^3
ρ_m : 3.0 g/cm^3

Table 5. Calculated porosities from average seismic velocities

Spread	V_a (m/s)	ϕ	V_w (m/s)	ϕ
1	1218	0.239359	1938	0.706192
2	1285	0.224001	2048	0.652148
3	1464	0.189864	1966	0.691862
4	1210	0.241306	2301	0.547458
mean	1294	0.222059	2063	0.645225

Table 5 shows the results of the porosity calculation. It is striking that while the porosity of the dry lava (air saturated) is in the range 0.19-0.24, a possible value, the water saturated lava shows a much greater porosity, 0.55-0.71. In other words, the velocity of the water saturated lava is much lower than expected. Equation (8) predicts 3700 m/s for water saturated porosity of 0.22. This is inconsistent with the assumption that the lava formation below the ground water level is similar to the lava above. In order to reconcile these data, the matrix velocity would have to be in the range 2000 to 2600 m/s, which is impossible for a basaltic lava.

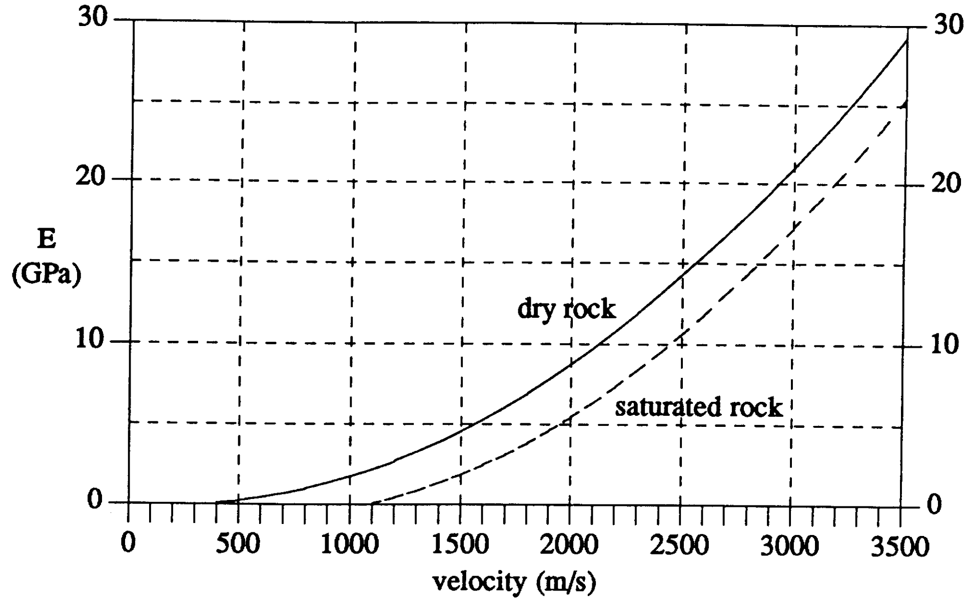

Figure 12. Young's modulus as a function of velocity in dry and water saturated rock, assuming that equation (11) is valid.

A possible explanation for this problem, is that the observed refracted phase is affected by a low velocity zone below the solid lavas. The material in this zone is probably lava breccia and clastic sediments. The long dominant wavelengths of the seismic signal, about 30 m are such that the wave could partly sample the low velocity layer, and thus give a velocity that is intermediate in value between the upper saturated lava and the lower sediments.

It is also possible that the lava above the water table is partly water saturated. This would possibly account for the relatively small velocity contrasts, but not for the large porosity of the saturated lower lava, as calculated in table 5. It could also be considered if the rock below the water table is not fully saturated. If there is gas production in the sediments below the lava, some gas could be trapped in the lava vesicles, and easily lower the velocity to the observed value.

The following approach has be chosen. We accept the above results for the dry lava as likely. This validates equation (11) in the case of dry lava, and this relation of seismic P-velocity and Youngs modulus is plotted in figure 11. The average velocity 1300 m/s corresponds to 3 GPa (10^9 Pascals), and the range in velocity of 700 to 2000 m/s corresponds to a range in Youngs modulus of 1-9 GPa. The figure shows also the relation for water saturated rock, assuming that equation (11) is also valid for these conditions. The modulus of the lava/sediments below 0-level would then be about 6 GPa, corresponding to 2100 m/s. If the velocity is underestimated, as discussed above, the value of the modulus is underestimated for the competent lava immediately below the ground water level.

The deep basement layer at a depth of 34 m below 0-level is probably another lava layer, probably denser. It has a velocity of 3100 m/s, which is a likely value for such rocks. The modulus for this layer is 18 GPa according to fig. 11.

The S-wave velocities must be calculated according to our basic assumption, which is the validity of the Poisson's relation, equation (3). This assumes the relation $V_s = V_p / \sqrt{3}$. By using the mean P-wave velocities in the previous two paragraphs, we calculate the S-wave velocities as 750 m/s for layer 1, 1212 m/s for layer 2, and 1790 m/s for layer 3.

6. REFERENCES

Christensen, N.I. and R.H. Wilkens, 1982. Seismic Properties, Density, and Composition of the Icelandic Crust Near Reydarfjördur. J.G.R., 87, 6389-6395.

Pálmason, G., *Crustal Structure of Iceland from Explosion Seismology*, 187 pp, Vísindafélag Íslendinga, Reykjavík, 1971

Wyllie, M.R.J, A.R. Gregory, and G.H.F Gardneer, 1958. An experimental investigation of factors affecting elastic wave velocities in porous media. Geophysics, 23, 459-493.

Bullen, K.E. *An Introduction to the theory of Seismology*, third ed., Cambridge, 1965.

Telford, W.M., L.P. Geldart, R.E. Sheriff, and D.A. Keys. *Applied Geophysics*. Cambridge 1976.